Energy Conversion and Management 198 (2019) 111778

Contents lists available at ScienceDirect

Energy Conversion and Management

journal homepage: www.elsevier.com/locate/enconman

Integrating wind, photovoltaic, and large hydropower during the reservoir refilling period

Xianxun Wang[a,b], Edgar Virguez[b], Jordan Kern[c], Lihua Chen[d], Yadong Mei[a,*], Dalia Patiño-Echeverri[b,*], Hao Wang[a,e]

[a] State Key Laboratory of Water Resources and Hydropower Engineering Science, Wuhan University, Wuhan, Hubei 430072, China
[b] Nicholas School of the Environment, Duke University, Durham, NC 27708, United States
[c] College of Natural Resources, North Carolina State University, Raleigh, NC 27695, United States
[d] College of Civil Engineering and Architecture, Guangxi University, Nanning, Guangxi 530004, China
[e] China Institute of Water Resources and Hydropower Research, Beijing 100038, China

ARTICLE INFO

Keywords:
Renewable energy
Integration
Refill operation
Multiobjective optimization
Pareto frontier
Complementary mechanism

ABSTRACT

Hydropower facilities are an ideal solution to complement the intermittent production of energy from wind and solar photovoltaic facilities in electric power systems. However, adding this task to the multiple diverse duties of a reservoir (e.g., flood mitigation, water supply, and power generation) poses a challenge related to pursuing multiple and sometimes conflicting objectives. This study proposes an approach for integrating hydro, wind, and photovoltaic power during a reservoir's refill period. Specifically, this approach simultaneously minimizes the fluctuation in the combined power output of these three resources and maximizes their combined power generation while adhering to the target reservoir's water levels. The proposed approach uses a multiobjective optimization model that prescribes a day-ahead optimal hourly operation for a hydropower facility in terms of spilled water, water stored in the reservoir, and water used for power generation, while meeting a daily target to refill the reservoir. The prescribed scheduling is then used as the input into a model that simulates the actual operations of the power system. This study focuses on a hydro-wind-photovoltaic system located in southwestern China, where the peak power generating capacity of the hydropower facility is ten percent larger than the combined installed capacity of the wind and solar power. The results show that by using the proposed model, the hydropower facility effectively smooths the fluctuations in the combined power output caused by variable wind and photovoltaic power and concurrently meets the reservoir replenishing targets under dry, moderate, or wet hydrologic scenarios. Furthermore, the trade-offs between power generation maximization and power fluctuation reduction were found to depend on two conditions: whether the reservoir is full, and whether the turbine is generating electricity at its maximum capacity. The hydro-wind-photovoltaic integration is more cost-effective when the reservoir is not full and the turbines are not generating electricity at their maximum capacity. When the reservoir is full, hydropower still has the ability to balance the wind and photovoltaic power without curtailment but tends to result in water spillage (22–402 m^3/s) and reductions in electricity generation (0.1–11.4 GWh per day). The proposed method for scheduling operations allows hydropower facilities to complement wind and photovoltaic power output, while meeting the target water levels during the refill period.

1. Introduction

Hydropower plays a central role as a source of energy storage and energy balance to supplement highly intermittent and variable energy sources such as wind and PV (photovoltaic) energy [1], which are the crucial components of future power systems with a high penetration of renewable energy [2]. However, many reservoirs have already been burdened with multiple responsibilities for flood prevention/mitigation, water supply, power generation, the provision of downstream water flows for environmental protection, and recreation [3]. Furthermore, hydropower operations are subject to changes in water availability, which has both seasonal and random variability [4]. Thus, managing a hydropower reservoir is already a complex mission [5], and adding the new task of complementing wind/PV power represents both a significant opportunity and an outstanding challenge [6].

The literature presents several studies on the modeling and analysis

* Corresponding authors.
E-mail addresses: ydmei@whu.edu.cn (Y. Mei), dalia.patino@duke.edu (D. Patiño-Echeverri).

https://doi.org/10.1016/j.enconman.2019.111778
Received 11 February 2019; Received in revised form 29 June 2019; Accepted 2 July 2019
Available online 11 July 2019
0196-8904/

of coordinated operations involving hydropower and wind/PV to achieve a range of objectives, including maximizing the benefits associated with power generation [7], profits [8], wind/PV integration [9], minimizing water consumption [10], power curtailment [11], power fluctuation [12], ramp rate [13], and the difference between generated power and load demand [14] or mitigating ecological consequences [15]. Nevertheless, most of the previous research on this topic fails to consider the full complexity of hydropower operations, and it does not account for the constraints associated with the seasonality of reservoir operations. The hydrological year is commonly divided into a dry season and a flood season. A flood season can be further partitioned into the following three subseasons: preflood season, primary flood season, and postflood season [16]. Varying hydropower operation policies are employed during these different periods of the year [17]. During the postflood season (i.e., refill period), when the probability of encountering a flood is low, water retention is also a primary obligation of the reservoir, to provide water resources during the dry season. Although less emphasis is placed on maximizing power generation, let alone helping to integrate the wind/PV power, the refill period is a phase when the reservoir has both the available water resources to generate power (e.g., ramping up) and the accessible reservoir storage capacity to store surplus water energy (e.g., ramping down without curtailment). Thus, there are profitable opportunities for hydropower to complement wind/PV power during the refill period.

Many studies involving reservoir regulation during the refill period have focused on formulating refill rules [18], determining refill probabilities [19], devising strategies for flood risk control [20], dynamically controlling the water level during the flood season [21] and other issues. Specifically, Liu et al. [18] proposed a model of single reservoir operation to derive refill rules aimed at maximizing power generation. Their results showed improvements in both the refill probability and the mean power production. Subsequently, Liu et al. [22] improved the refill operation model by considering multiple objectives in terms of minimizing the flood risk and spilled water as well as maximizing the power generation and refill probability. A case study on the Three Gorges Reservoir showed that these objectives were achieved without decreasing the flood control standard. Regarding the joint refill operation of cascaded reservoirs, Li et al. [20] proposed a method that combined the impoundment principle [23] with the K-value discriminant method to determine the optimal impoundment sequence of cascaded reservoirs. Furthermore, Zhou et al. [24] proposed joint refill rules for cascaded reservoirs by combing flood control risk and utilization benefits (e.g., power generation and refill probability). Their results indicated that the tradeoff between flood control and water utilization could also be managed in the cascades of reservoirs. The pressure to challenge the management of refill operations is increasing with the formation of clusters of extremely large storage reservoirs [23]. Nevertheless, to the best of the authors' knowledge, the integration of hydropower wind/PV power with refill operations has not been investigated. The major challenge is to integrate the renewable energy and refill the reservoir simultaneously. This is difficult because both tasks have specific water level requirements that can sometimes be conflicting. To fill this gap and overcome this challenge, this paper proposes a model of hydro-wind-PV power (HWPP) integration during the refill period and analyzes its performance in a case study.

China, already a world leader in clean energy in terms of both total renewable installed capacity and renewable electricity generation [25], will increase the share of nonfossil fuels for use in primary energy consumption to approximately 20% by 2030 [26]. A renewable power project with a total combined capacity of 60 GW has been designed in the Yalong River basin to demonstrate the integration of hydro-wind-PV power, and at completion, these energy sources will make up the largest HWPP cluster in China [27]. This paper addresses the case of Ertan, which is the major hydropower facility in the basin and one of the largest plants hydropower in China, with an installed capacity of 3300 MW and a large reservoir of $3370 \times 10^6\ m^3$ that takes several weeks to refill. This hydropower plant is representative of similar facilities that periodically need to refill their reservoirs. This study presents a case study of Ertan's combined hydropower, wind, and PV resources to illustrate the rationality and potential of a modeling approach to using the power balancing and storage capabilities of hydropower facilities optimally during their refill period. The novelty of this study is that it proposes an approach to use hydropower effectively to complement wind/PV power while meeting the water level constraints that are present during the refill period. It proposes a new way of dispatching the hydropower facility to integrate wind/PV power at an hourly scale while simultaneously meeting daily target water levels.

The remainder of this paper is organized into the following sections: 1) a description of the modeling approach; 2) details of the mathematical function measuring the temporal variation in power output; 3) the solution algorithm of the model; 4) the results and discussion of the proposed coordination mechanism of the HWPP system and its implications for the Ertan project; and 5) the conclusions.

2. Dispatching the hydropower facility to meet target water levels

To complement the fluctuating power output from wind/PV sources and produce a stable source of electricity, hydropower generators should be dispatched in a reciprocal manner. Fig. 1 presents two examples of when hydropower is dispatched to complement wind/PV power. During the refill period, which usually lasts several weeks, the reservoir gradually impounds water based on a daily, weekly or monthly schedule. Accordingly, the water level of the reservoir increases daily, weekly, or monthly. Barring any requirements for specific water discharges (e.g., to cause an artificial flood), hydropower can be dispatched with relative freedom as the reservoir water level reaches its scheduled targets. Therefore, the objectives to complement wind/PV power and to impound water in the reservoir can be simultaneously achieved by dispatching the hydropower in a reciprocal manner while constraining the target water level.

As long as the hydropower production is reciprocal to the wind/PV power generation (i.e., when the wind or PV sources generate high/low production, the hydropower generates low/high production) the complementarity of these power sources is achieved, even if the

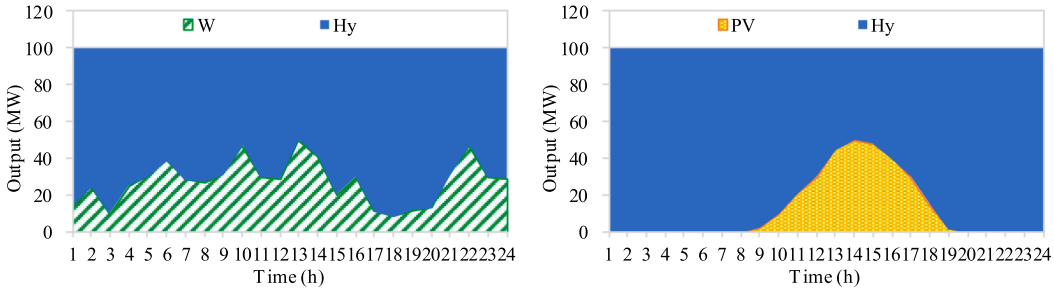

Fig. 1. Reciprocal output processes of hydropower and wind/PV power (W refers to wind power, Hy refers to hydropower, and PV refers to PV power).

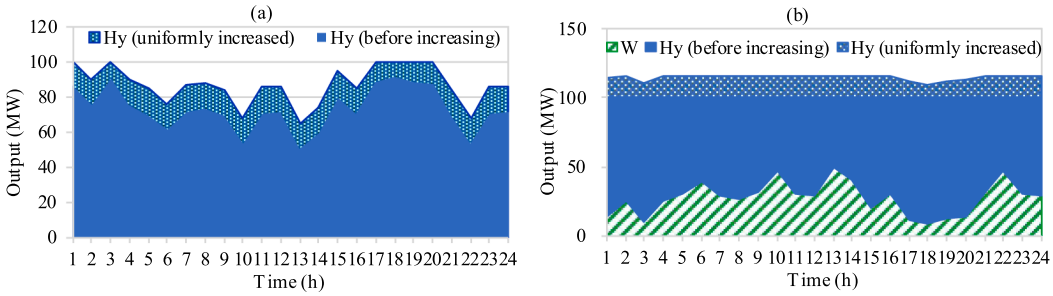

Fig. 2. Diagram illustrating a uniform increase of 15 MW in hourly hydropower output when considering an upper boundary imposed by the installed capacity (e.g., 100 MW): (a) hydropower dispatch processes before and after increasing the power output and (b) wind power output combined with hydropower output processes in the left panel.

hydropower output is uniformly higher or lower. Thus, the total hydropower production over the dispatch horizon can still be increased or decreased to reach the target water level without compromising its ability to balance the wind and PV power production. The procedure for dispatching hydropower to meet the target water level is as follows:

Step 1: Calculate the reservoir's water level at the end of the dispatch horizon (H_{end}) resulting from the initial hydropower dispatch process (i.e., the *Hy* dispatch process before increasing/decreasing, as shown in Figs. 2 and 3). The initial hydropower output process is set to be reciprocal to the output of wind/PV power, but its water level at the end of the dispatch horizon does not necessarily meet the target water level.
Step 2: Calculate the gap (H_{gap}) between the target water level (H_{target}) and H_{end}. $H_{gap} = |H_{end} - H_{target}|$.
Step 3: If H_{end} is higher than H_{target}, uniformly increase the hydropower output process, ensuring that the increased output does not exceed the maximum power generating capacity of the hydropower facility; otherwise, uniformly decrease the hydropower output, ensuring that the decreased output is above the minimum power generation level considered safe for the hydropower facility. As shown in Fig. 2, the maximum hydropower generation capacity of 100 MW implies that at 3:00 and from 17:00 to 20:00, the power output cannot be greater than this amount. Fig. 3 shows that the minimum hydropower level of 35 MW implies that at 6:00, 10:00, 13:00, 14:00, and 22:00 the hydropower output cannot be lower than this amount.
Step 4: Calculate H_{end} and H_{gap} with the adjusted process obtained in step 3.
Step 5: If H_{gap} is less than a prespecified criterion (e.g., 0.01 m), then stop, because at this point, the hydropower output process that meets the required target water level is obtained. If not, proceed.
Step 6: If the H_{end} is higher/lower than the H_{target} and there is space to increase/decrease the amount of dispatched hydropower, then go to step 3. If not, stop and use the optimal hydropower dispatch process for which the water level at the end of the dispatch horizon is closest to the target water level.

3. Model of hydro-wind-photovoltaic integration during the refill period

An exploration of the HWPP integration during the refill period allows for a better understanding of the ability of hydropower to help meet two competing objectives, namely (1) minimizing power fluctuations from the combined wind/PV power projects and (2) maximizing the total power production for the HWPP project. To complement the fluctuating wind/PV power output, the hydroelectric reservoir must (1) use water in the reservoir to generate more power (probably losing the water head) or (2) reduce power generation, either by storing inflows, or, when that is not possible due to lake levels, "spilling" water (i.e., discharging water downstream without generating electricity). The loss of the water head and the spillage of water leads to trade-offs between minimizing power fluctuations and maximizing power generation. This trade-off was noted in a previous study [12] that examined the case of a prefectural-level power grid in southwestern China.

The primary contribution of the model proposed in this work is that the temporal horizon considered here is the period when the reservoir must be filled. This consideration imposes additional constraints and requires an improved technique for hydro-wind-PV integration. The primary constraint of the HWPP integration model during the refill period is set by the requirement to meet a target water level at the end of the daily dispatch horizon. Due to safety and economic considerations within power system operations, this model also considers two objectives, namely, minimizing the total power output fluctuation and maximizing the total power production. Its results illustrate the mechanism of HWPP integration during the refill period. It is assumed that hourly HWPP system operations are planned the day ahead to optimize the two objectives simultaneously. The model finds the optimal day-ahead schedule of the HWPP system by considering the forecast for the wind speed, solar radiation, and water inflows to the reservoir. Then, in

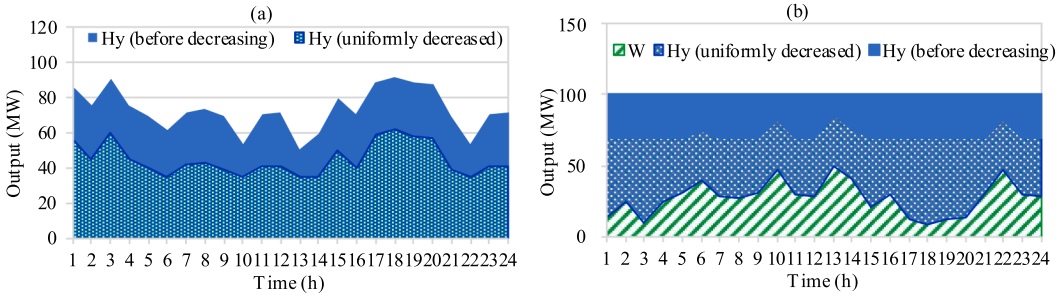

Fig. 3. Diagram illustrating a uniform decrease of 30 MW in hourly hydropower output when considering a lower boundary set by the minimum permissible output (e.g., 35 MW): (a) hydropower dispatch processes before and after decreasing the power output and (b) wind power output combined with hydropower output processes in the left panel.

real time, the hydropower facility operates as needed to adjust to the actual conditions in terms of the wind speed, solar radiation and water inflows, while striving to meet the power production schedules planned the day ahead. This modeling framework represents the situation of a power producer that commits to injecting a set amount of power generation from its HWPP system into the grid one day ahead, for each hour over the next 24-hour period. The deviation in the water level at the end of the day is caused by a forecast error and will be balanced during the subsequent day-ahead plan, and hence it is avoided to the extent possible. The solution to the multiobjective problem solved in the day-ahead model is a Pareto frontier (a set of nondominated solutions, each of which represents a situation in which no objective can be improved without sacrificing at least one other objective). Pareto frontiers are identified using an evolutionary algorithm called the nondominated sorting genetic algorithm II (NSGA-II [28], described in Section 4).

3.1. Objective function

There are two competing objective functions involved in this study, that is, minimizing HWPP output fluctuations and maximizing HWPP power generation.

3.1.1. Minimizing output fluctuation

This study employs the Mei-Wang Fluctuation index [29], which combines the standard deviation and rotation angle to quantify the power output fluctuation in the HWPP system. Other indices such as the Richards-Baker Flashiness index [30], the first-order difference, and the standard deviation are also commonly used to quantify the variability. However, a comparison of these indices (Section 3.1 in [29]) shows that the Mei-Wang Fluctuation index has better performance by accounting not only for the quantitative variation but also for the contour variation. In recent literature, the Mei-Wang Fluctuation index has been employed to quantify the variability in power outputs of PV-wind-pumped storage system [31], PV-wind system [32] and wind-PV-hydro system [33] effectively.

In the Mei-Wang Fluctuation index, the rotation angles associated with a time series of the power output can be observed in a two-dimensional graph of power output vs time (Fig. 4). For each level of power output P_i, there is an associated power output rotation angle that depends on the magnitude of the power output at one time instance relative to the trend observed during the immediately previous periods. In this way, the power output rotation angle captures the magnitude of sudden fluctuations. In addition, using this index, one large rotation angle is weighted to a greater degree than several small rotation angles; this type of event might be associated with the need to start up and/or shut down plants in a power system, which can be a considerable expense for system operators. In the subsequent research [34], this weighting is achieved by taking the exponential function of each angle before adding them up. In this study, the advanced Mei-Wang Fluctuation index [34] is employed to characterize the output fluctuation. The objective of minimizing the output fluctuation of the HWPP system is formulated as shown in Eqs. (1)–(7).

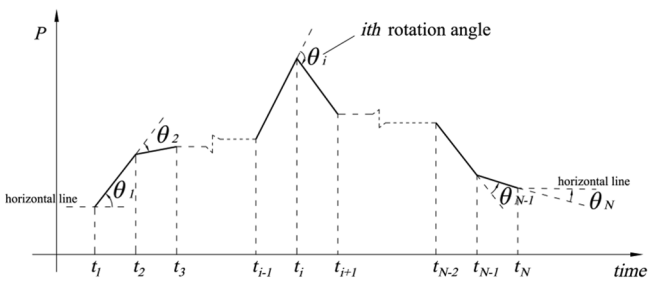

Fig. 4. Schematic diagram showing the rotation angle of the output progress.

$$\min_{\lambda_i (i=1,2,\ldots,N)} (\alpha \times \beta) \tag{1}$$

$$\alpha = \sqrt{1/N \times \sum_{i=1}^{N} (P_i^{co} - \bar{P}^{co})^2} \tag{2}$$

$$\beta = \sum_{i=1}^{N} (exp(\theta_i) - 1) \tag{3}$$

$$\theta_i = \begin{cases} \arctan |k_i| & i = 1 \text{ or } N \\ |\arctan k_i - \arctan k_{i-1}| & 2 \le i \le N - 1, \text{ and } k_i \times k_{i-1} \ge 0 \\ \arctan |k_i| + \arctan |k_{i-1}| & 2 \le i \le N - 1, \text{ and } k_i \times k_{i-1} < 0 \end{cases} \tag{4}$$

$$k_i = \begin{cases} (P_{i+1}^{co} - P_i^{co})/(t_{i+1} - t_i) & 1 \le i \le N-1 \\ k_{N-1} & i = N \end{cases} \tag{5}$$

$$P_i^{co} = P_i^{Hy} + P_i^{W} + P_i^{PV} \tag{6}$$

$$P_i^{Hy} = \lambda_i \times P_i^{Hy,exp} \tag{7}$$

where subscript i refers to the time interval; N is the total number of intervals in the time horizon; α is the standard deviation of P_i^{co} [MW]; β is the summation of the exponential value of θ_i [radian]; P_i^{co} is the total power output of the HWPP system in the ith interval [MW]; $\bar{P}^{co}$ is the average value of P_i^{co} during the time horizon [MW]; θ_i is the rotation angle of P_i^{co} in the ith interval as shown in Fig. 4 [radian]; k_i is the gradient between P_i^{co} and P_{i+1}^{co} [MW/h]; P_i^{Hy} is the hydropower output in the ith interval [MW]; the superscript Hy refers to hydropower; P_i^{W} is the wind farm power output in the ith interval [MW]; the superscript W refers to the wind power; P_i^{PV} is the PV power output in the ith interval [MW]; the superscript PV refers to PV power; $P_i^{Hy,exp}$ is the maximum output of hydropower in the ith interval, namely, the largest output that could be generated with the inflow and the water in the reservoir [MW]; and λ_i is the ratio of the hydropower output in the ith interval, which is the variable in the model and ranges from 0 to 1. The detailed definitions and calculations of these parameters can be found in [29].

3.1.2. Maximizing power generation

The objective of maximizing the power generation is expressed as:

$$\max_{\lambda_i (i=1,2\ldots,N)} \left(\sum_{i=1}^{N} (P_i^{co} \times \Delta t) \right) \tag{8}$$

where Δt is the temporal length of single time interval [h].

3.2. Constraints

The model of HWPP integration during the refill period has three types of constraints, namely the natural resources (e.g., inflow, wind speed, and solar radiation), the power grid (e.g., the power grid topology and transmission capacity), and the power station (e.g., the water balance and ramping ability). In this paper, the lack of specific data on the power grid in the study area prevents the consideration of the power grid constraints. It is assumed that there is enough electricity demand to consume all the power produced by the HWPP. Details on the power grid constraints and their influence on HWPP integration can be found in [12].

(1) Hydropower

$$|H_{target} - H_{end}| \le H_{gap}^{ctr} \tag{9}$$

$$V_i + (Q_i^{in} - Q_i^{out}) \times \Delta t = V_{i+1} \tag{10}$$

$$Q_i^{out} = Q_i^{out,turbined} + Q_i^{out,spilled} \tag{11}$$

$$P_i^{spilled} = P_i^{Hy} \times Q_i^{out,spilled} / Q_i^{out,turbined} \tag{12}$$

where H_{target} is the target water level of the hydropower reservoir at the

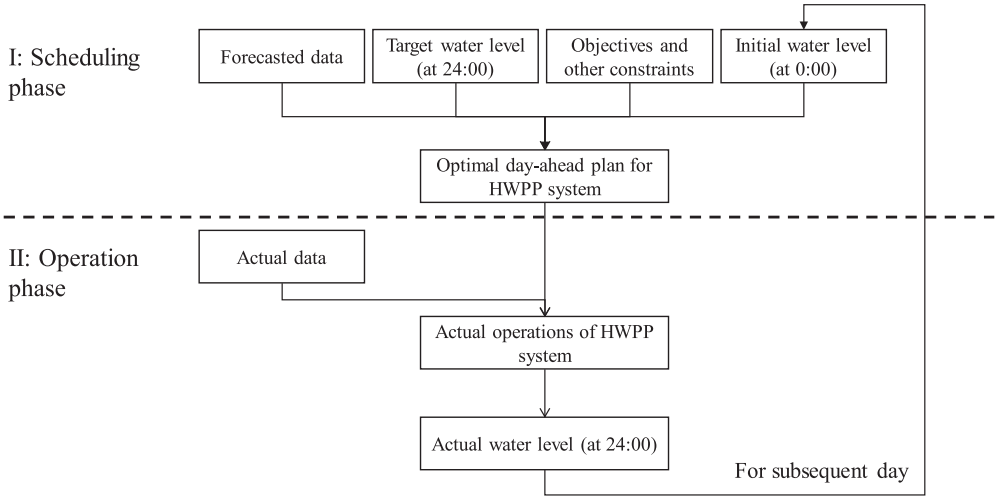

Fig. 5. Simulation of HWPP system scheduling and operation.

end of the dispatch horizon [m]; H_{end} is the water level of the hydropower reservoir at the end of the dispatch horizon given as a result of the optimization model [m]; H_{gap}^{ctr} is the control value of the gap between H_{target} and H_{end} [m]; V_i is the volume of water stored in the reservoir at the beginning of the ith interval [m^3]; Q_i^{in} is the inflow of the reservoir in the ith interval [m^3/s]; Q_i^{out} is the outflow of the reservoir in the ith interval [m^3/s]; $Q_i^{out,turbined}$ is the outflow from the reservoir used to generate hydroelectric power (i.e., "turbined flow") in the ith interval [m^3/s]; $Q_i^{out,spilled}$ is the spilled outflow from the reservoir, which is not used to generate power (i.e., discharged through the spillway) in the ith interval [m^3/s]; and $P_i^{spilled}$ is the hydroelectric power that could have been generated with the water spilled during the ith interval [MW].

Note that regardless of whether water is discharged through the power plant (i.e., turbined outflow) or discarded through the spillway (i.e., spilled outflow), the water quantity that passes downstream is not altered. However, spilling water can be limited by environmental regulations on the flows downstream of some hydropower reservoirs [35]. Because spilling large volumes of water can cause high levels of dissolved gases that are harmful to fish [36] while allowing the water to pass through the turbines to generate power does not cause this problem, in some power systems (e.g., the Federal Columbia River Power System), the operators will strategically curtail the wind/PV power and not the hydropower.

(2) Wind power

$$P_i^W = \begin{cases} 0, & WS_i < WS_{cut-in} \text{ or } WS_i \geq WS_{cut-out} \\ gen(WS_i), & WS_{cut-in} \leq WS_i < WS_{cut-out} \end{cases} \quad (13)$$

where WS_i is the wind speed in the ith interval [m/s]; WS_{cut-in} is the minimum wind speed required for power generation at this wind turbine [m/s]; $WS_{cut-out}$ is the maximum wind speed at which this wind turbine can generate power [m/s]; and $gen(*)$ is a function that outputs the amount of electric power production of the wind turbine for a given wind speed.

(3) PV power

$$P_i^{PV} = IC^{PV} \times (R_i/R_{stc}) \times [1 + \varphi_{PV} \times (T_i - T_{stc})] \quad (14)$$

where IC^{PV} is the installed capacity of PV [MW]; R_i is the actual intensity of solar radiation in the ith interval [W/m^2]; R_{stc} is the solar radiation intensity under the standard test conditions, equivalent to 1000 W/m^2; φ_{PV} is the temperature coefficient of power output from the solar cell module ($-0.35\%/^{\circ}C$); T_i is the actual temperature of the module in the ith interval [°C]; and T_{stc} is the temperature under the standard test conditions (25 °C [7]).

4. Solution algorithm

Typically, reservoir refill periods last from several weeks to several months. As mentioned above, in this study, the scheduling and operation of the HWPP system are conducted hourly (i.e., operation resolution), for one day (i.e., operation horizon) at a time, which is repeated for the duration of the refill period. This combination of the resolution and the time horizon results in an acceptable computing time. Using a more granular resolution or longer planning horizons will increase the computation time and do not alter the conclusions of this study. It is assumed that the power output fluctuations over longer time periods can be better managed when starting up, shutting down, or ramping the power output up and down from conventional generation resources. The "refilling" stage is the period between the day when the reservoir starts to refill and the day when the reservoir is fully filled. The "filled" stage is any day after that point. In other words, the refill period is divided into a refilling stage and a filled stage.

Because there are errors in the day-ahead forecasts of the inflow, wind speed and solar radiation, the operation of hydropower in real time must be adjusted to meet the power production schedules. For this reason, this study simulates the daily operations of the HWPP system in two phases, the scheduling phase and the operation phase. During the scheduling phase, the forecast runoff, wind speed, and solar radiation are used to find the optimal plan (i.e., day-ahead schedule) for operating the HWPP system; during the operation phase, the actual conditions (i.e., forecast data + forecast error on wind, solar, and water flow) are considered. During the scheduling phase, the operations are planned to achieve the power production maximization and power fluctuation minimization objectives while meeting the water target level set for the end of the day and other operational constraints. In real time, the hydropower plant is dispatched to generate the power production using a day-ahead schedule, and hence, due to forecast errors, there may be a difference between the target water level of the reservoir at hour 24 and the real water level at that time. This difference will be balanced during the subsequent day. The two phases are illustrated in Fig. 5.

With rapid improvements in computer performance, heuristic algorithms such as the genetic algorithm (GA) and particle swarm optimization (PSO) are increasingly used to solve hydropower system or energy system optimization problems [37]. The HWPP scheduling model is multiobjective and nonlinear, so it is solved with the nondominated sorting genetic algorithm II (NSGA-II [28]), which has been frequently applied to solve multiobjective problems [38] because of its

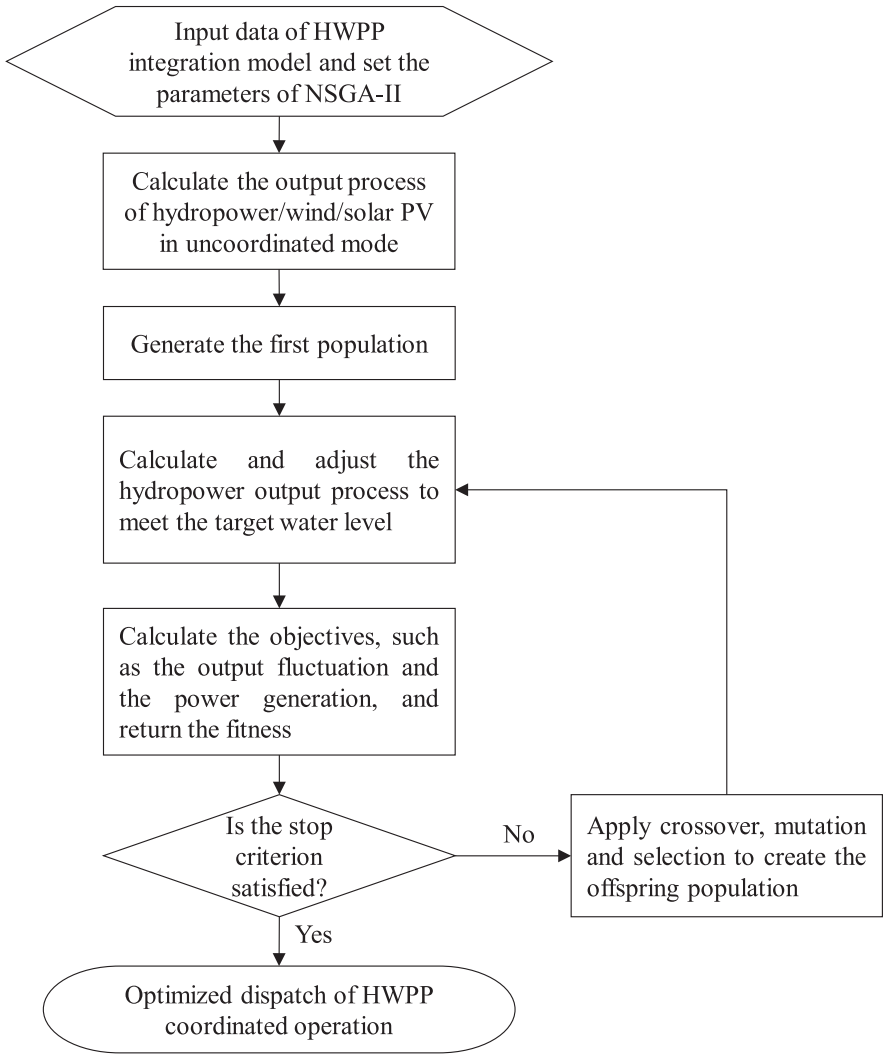

Fig. 6. Flow chart of the solution algorithm.

low complexity, fast convergence and uniform distribution of the Pareto frontier. In this study, the multiobjective optimization toolbox in MATLAB based on NSGA-II [39] is employed to determine the optimal coordination of the HWPP system and to obtain the Pareto frontier between the output fluctuation and the power generation (See Fig. 6).

The solution process is completed in six steps as described below:

Step 1: Simulate the independent/uncoordinated power generation process of the hydropower/wind/PV facilities. The uncoordinated operation of the hydropower facility is dispatched according to its operational rule curves as shown in Fig. A.1, Appendix A. The power generation process of the wind/PV facilities is calculated according to the wind/solar resources, as shown in Figs. A.3 and A.4 in Appendix A. The water level of the reservoir that is determined at the end of the day is the target water level H_{target}.

Step 2: Randomly generate an initial solution set (in the jargon of genetic optimization algorithm, this is called "the first population") of λ_i for $i = 1 \ldots N$ values, which are the decision variables of the model (i.e., a value from 0 to 1).

Step 3: Calculate the hydropower production corresponding to the values of λ_i and adjust the hydropower output process to meet the required H_{target} by uniformly increasing/decreasing production as noted earlier.

Step 4: Evaluate the quality of the solution (which is called "fitness of the current population' in the terminology of the genetic optimization algorithm). The fitness value (f1, f2) is calculated where f1 is the fluctuation in the combined power output from the hydro-wind-PV facilities and f2 is the total power generation corresponding to the two objective functions.

Step 5: If the stop criterion of NSGA-II (i.e., the number of iterations/generations) is satisfied, then stop and export the final optimal coordinated dispatch. Otherwise, proceed.

Step 6: Generate an alternative solution (i.e., generate "the offspring population" by using methods such as crossover, mutation, and selection) and go to step 3.

The flow chart of the solution algorithm is displayed below:

5. Case study

This study presents the case of the Ertan hydropower station located in southwestern China with a wind farm and PV power station that are planned for construction in the same region.

5.1. Data

Ertan hydropower station is one of the largest hydropower stations in China, with 3300 MW of installed capacity, 3370 $\times$ 10^6 m^3 of water

conservation storage (i.e., the portion of a reservoir's live storage that is normally conserved for beneficial use at-site or downstream, but does not include any live storage space reserved exclusively for flood control [40]) and 46.5 GWh annual mean daily power production. Due to its large storage capacity, a full reservoir would allow the hydropower facility to generate power at its full installed capacity for 15 days.

Usually, the Ertan reservoir starts to refill in late September or early October. In this study, it is assumed that the hydropower reservoir refill operation starts on October 1st and that the installed capacity of wind and PV power are 1000 MW and 2000 MW, respectively. This study addresses the period from October 1st to 31st and focuses on two stages, the refilling stage and the filled stage. The refilling stage starts on October 1st and ends on the day when the reservoir is fully refilled, while the filled stage refers to all the subsequent days until October 31st.

Three different inflow time series with insufficient, medium, and abundant water resources (i.e., three hydrologic scenarios) are tested to explore the impacts of the year-to-year differences in stream-flow availability. These time series correspond to observations during the month of October over three different years that were selected from over a period of 20 years, and hence they are representative of the hydrologic conditions in the region. The optimization of HWPP integration is performed day by day. Under each scenario, there are 31 optimizations, each of which is used for finding the values of 24 variables. The optimization is solved by using the following parameters for the NSGA-II: the population size is 100, the crossover rate is 0.5, the mutation rate is 0.01, and the generation number is 50. The errors in the day-ahead forecast on the availability of the three natural resources, namely, wind, PV and water inflow, are assumed to follow a normal probability distribution according to recent improvements in forecasting techniques (e.g., artificial neural networks [41], support vector machine [42], *meta*-heuristic techniques [43], and extreme learning machine [44]). A summary of all the data used here and the assumptions regarding the forecast errors can be found in Appendix (A).

5.2. Results and discussion

The potential use of hydropower to complement wind and PV production is examined by comparing the operations under two operation modes, an uncoordinated mode and a coordinated mode. In the uncoordinated operation mode, hydropower is dispatched without any consideration of the energy produced by wind and PV; in the coordinated mode, hydropower is dispatched as needed to complement the wind and PV power while meeting its technical constraints.

5.2.1. Uncoordinated operations

When the operations of the hydropower facility are not coordinated with the wind/PV power resources, the reservoir is operated in a conventional manner; it may run as a peaking, intermediate, or base-load power source. In the uncoordinated mode, it is assumed that during the refilling stage, Ertan runs continuously to supply base load power, which is dispatched according to the operational rule curves that specify the amount of power production that can be generated for different water levels in the reservoir (as shown in Appendix A); during the filled stage, Ertan generates power output according to the runoff (i.e., run-of-river hydropower). As mentioned above, three inflow time series with different water amounts (5.80–7.74 billion m^3 over a 1-month period) are used to study the refill processes under various hydrologic conditions. Three scenarios with insufficient, medium, and abundant water resources are considered (called Scenarios 1, 2 and 3). The results of the reservoir water level and the power output of the HWPP system in the uncoordinated mode are displayed in Figs. 7 and 8.

The refill stage starts on October 1st and ends on the day when the reservoir is fully refilled (i.e., when the reservoir water level reaches 1200 m, as shown in Fig. 7(b)). Due to differences in water availability across Scenarios 1, 2, and 3 (5.80, 6.36, and 7.74 billion m^3, respectively), the duration of the refill stage decreases from 30 days to 27 days and 16 days, respectively (as shown in Fig. 7(b)). The reservoir water levels displayed in Fig. 7(b) are then used as constraints (i.e., daily target water level) in the HWPP integration.

5.2.2. Coordinated refill

When the generation of the hydropower plant is scheduled to complement the wind/PV power, it is said to be operating in a "coordinated refill" mode. During the coordinated refill mode, the reservoir water level at the end of each day is required to be the same as what is obtained in the uncoordinated mode (as shown in Fig. 7(b)). Within the day, the optimization of the HWPP system is performed on an hourly basis to optimize its two objectives.

5.2.3. Cooperation mechanism

Pareto "nondominated" solutions for the two objectives of the scheduling optimization are displayed in Appendix B. To explore the dam's ability to smooth the total HWPP power output, the Pareto solution with the smallest power fluctuation is selected for further comparison between the uncoordinated and coordinated refill modes.

Fig. 8 shows that within any given day, the total output of the HWPP system in the coordinated refill mode is smoother than it is in the uncoordinated mode. This is because under the coordinated refill mode, the hydropower facility is deliberately scheduled to complement the wind and PV power production and dispatched to maintain this schedule. Using the first day as an example (displayed in Fig. 9), in the coordinated refill mode, the hydropower output is purposely ramped up from 571 MW to 1833 MW to complement the wind and PV power, whereas in the uncoordinated mode, its output has a constant value of 1028 MW.

Regarding the water level, the hydropower schedule under the coordinated refill mode results in a water level that is equal to the target water level (1157.91 m) at 24:00; however, actual hydropower operations result in a water level of 1157.82 m at 24:00, which is 0.09 m lower than the target water level. This deviation results from the forecast error and depends on the prediction accuracy. The deviation from the water level targets is addressed during the scheduling process on the subsequent day, which produces a plan to meet the target. Under Scenario 1, the deviation ranges from −0.22 to 0.05 m, which is a small amount compared to the 45 m target for the water level required for the refill. Similar results are observed under Scenarios 2 and 3.

These results illustrate that hydropower can be dispatched to complement the wind/PV power while closely following its daily impoundment target during the refill period. Similar outcomes under dry, moderate, or wet hydrologic scenarios show the robustness of the proposed approach. Because the coordinated operation of the HWPP system is performed within its temporal horizon (one day, in this study), there is an abrupt ramping between two adjacent horizons (as shown in Fig. 8, 457 h and 481 h). Adding a ramping limitation between two adjacent horizons can fix this mismatch.

The outcomes of the coordinated operation show that with the optimal dispatch of fast ramping and flexible hydropower, the total output of the HWPP system can be stable and sometimes even flat, mimicking the power output of a base load plant. This result suggests a promising future for systems with high penetration of intermittent renewables and hydropower [45], a possible solution to the need for the ramping up capability that is now traded as a product in organized electricity markets in the United States [46].

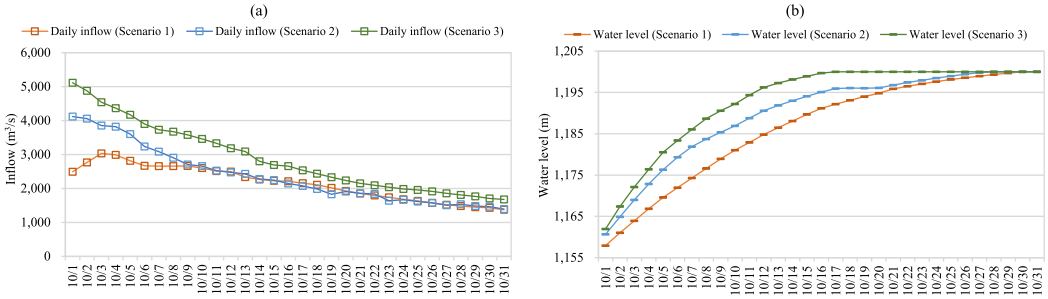

Fig. 7. Refill process for hydropower in the uncoordinated mode: (a) the average daily inflow of the reservoir and (b) the water level of the reservoir at the end (24:00) of each day.

5.2.4. Trade-offs during the refilling and filled stages

Previous research [12] notes that smoothing the total output from HWPP systems causes a conflict with the objective of maximizing power generation. Using the results of this study, a comparison of the Pareto frontiers for the refilling and filled stages sheds light on this trade-off.

Six Pareto frontiers are displayed in Fig. 10 (additional frontiers are displayed in Appendix B). The top row shows the results during the refilling stage; the bottom row shows the results during the filled stage. The columns (left to right) show the results for Scenarios 1, 2, and 3. The results during the refilling stage (first row) indicate that when the reservoir is not full, a slight reduction in power generation is enough to improve the power smoothing significantly. This is because the penalties are only 0.15, 0.21, and 0.20 GWh under Scenarios 1, 2, and 3 respectively, which represent 0.3%, 0.5%, and 0.5% of the annual mean daily power production of the Ertan reservoir (i.e., 46.5 GWh per day). However, in the second row, when the reservoir is already full, smoothing the power output leads to remarkable reductions in power production of 11.7, 15.0, and 15.5 GWh under Scenarios 1, 2, and 3, respectively, which represent 25.2%, 32.3%, and 33.3% of the annual mean daily power production of the Ertan reservoir. This is because the hydropower output is ramped down to offset increases in wind/PV production completely when the reservoir is already full, or because when the reservoir storage capacity is insufficient, the water has to be spilled, reducing opportunities to generate electricity later. This finding demonstrates that during both the refilling and filled stage (i.e., before and after the reservoir is full), hydropower can complement the wind/PV power by smoothing the total output fluctuation at the expense of reduced power generation. However, it is more economical to coordinate the HWPP operations during the refilling stage when the reservoir has the available storage capacity.

5.2.5. Storage capacity and electricity generating capacity

In addition to the storage capacity of the reservoir, the mean power output being generated by the hydropower plant during a given time (e.g., the mean daily power output) also affects the integration of the HWPP. The storage capacity reflects the amount of energy that can be stored or provided in the form of water in the reservoir, while the mean power output relates to the amount of power production that can be produced within a given time. Fig. 11 illustrates a partition of all the possible situations combining the reservoir storage level at the beginning of the operation horizon (e.g., full or not full) with the mean power output during the operation horizon (e.g., equal to the maximum power output or not).

In Situations 1 and 3, when the reservoir is full, and hence there is no capacity to store any water energy, a reduction in hydropower generation results in spillage (as shown in Fig. 12, from 385 h to 552 h). In Situation 2, when the reservoir is not full, the water that cannot be used (because the power production is already at maximum capacity)

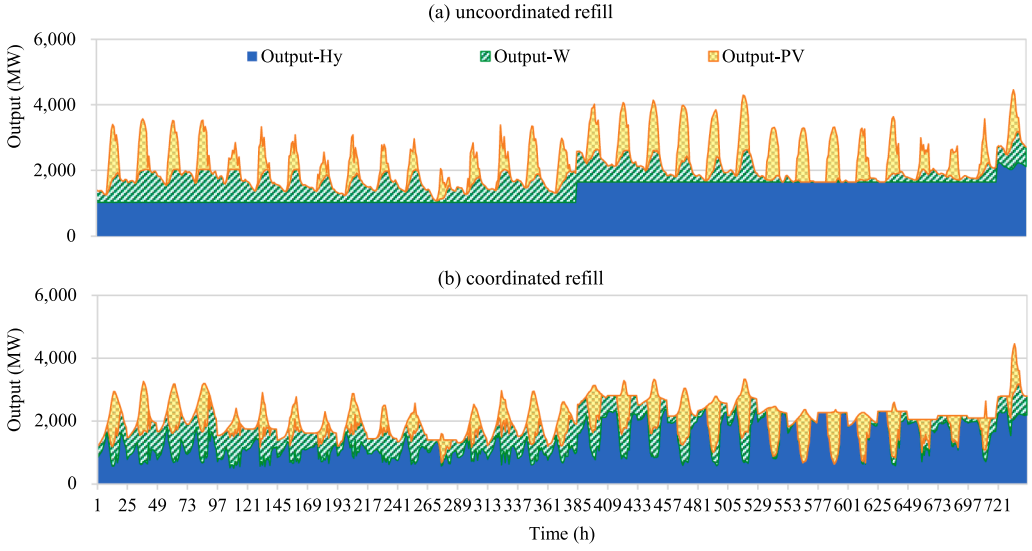

Fig. 8. Output of the HWPP system under Scenario 1.

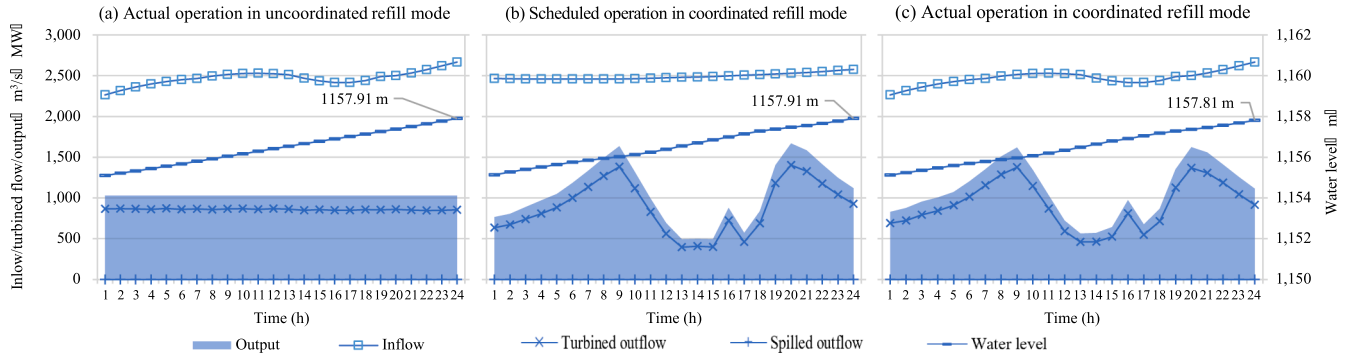

Fig. 9. Intraday operation of hydropower on the 1st day.

can be stored (as shown in Fig. 12, from 193 h to 240 h). In this case, the hydropower cannot complement the wind/PV power unless its output is decreased, which would either violate the constraint of the target water level by over-refilling the water in the reservoir (Fig. 13(d)) or contravene the common routine of reservoir operation by spilling the water when the reservoir is not full. In Situation 4, there is both sufficient storage capacity and the ability to alter the power output. This means that if the hydropower production is reduced, water can be stored, and if needed, the hydropower production can be increased (as shown in Fig. 13(h)). Thus, Situation 4, in which hydropower can complement wind/PV power without any spillage, is the best situation of the four.

5.2.6. Water spillage and associated forgone hydropower

When the reservoir is full, smoothing the fluctuating output of wind/PV power through the coordinated operation of the hydropower plant may result in water spillage (i.e., water is passed downstream without generating power). Across the three scenarios tested here, water spillage occurs under Scenario 3 when the inflow is abundant. The spilled outflow ranges from 22 m^3/s to 402 m^3/s and the daily power curtailment ranges from 0.1 GWh to 11.4 GWh. The results show that in a full reservoir situation, employing hydropower to smooth the varying wind/PV power requires a significant reduction in hydropower production and the spilling of large volumes of water, which can cause environmental problems (e.g., harmful concentrations of dissolved gases). This finding confirms that the integration of the HWPP at the end of the refill period, when the reservoir is full, should be discouraged.

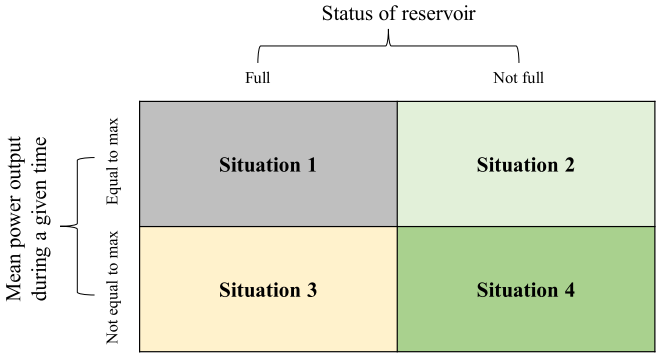

Fig. 11. Four possible situations of hydropower reservoir operation: when the mean power output is equal to the maximum power output (i.e., installed capacity), the hydropower plant cannot produce more power at that time, regardless of the reservoir's water level; when the reservoir is full, the water inflow must be spilled or used to generate power.

6. Conclusion

Hydropower facilities are ideal components of power systems with large shares of intermittent power production from wind and PV

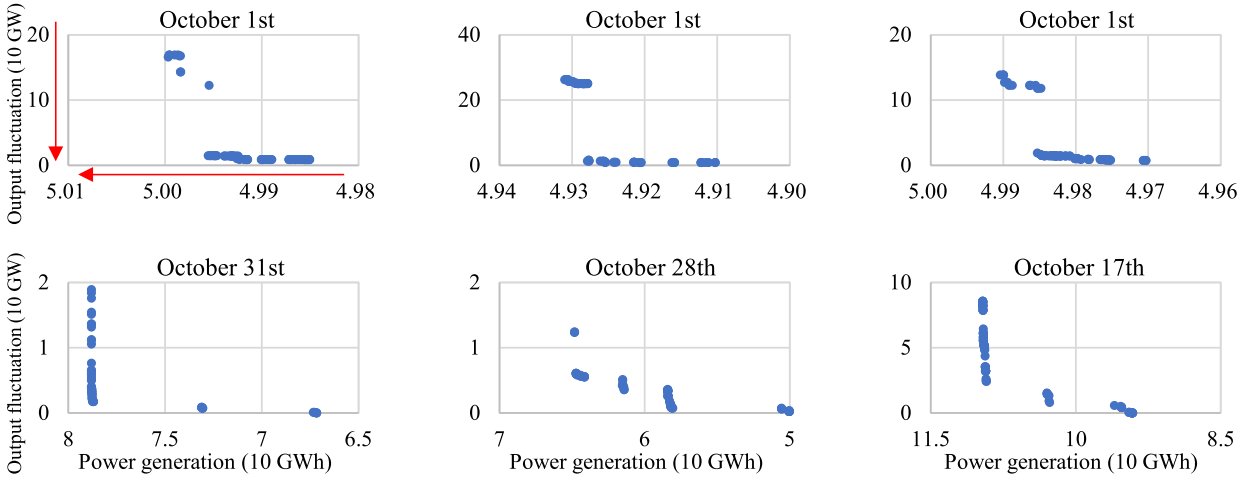

Fig. 10. Pareto frontiers of coordinated HWPP optimization during the refilling and filled stages: the first/second rows show the results for the refilling/filled stage, while the first, second, and third columns show the results for Scenarios 1, 2, and 3, respectively; the red arrows point to the preferred values of the objectives.

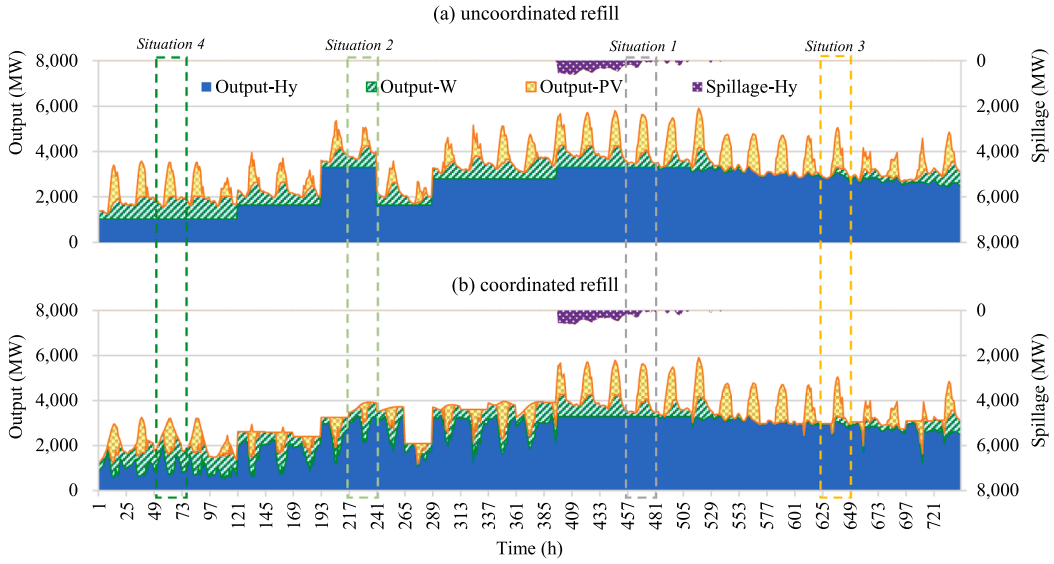

Fig. 12. Output of the HWPP system under hydrologic Scenario 3. The zones for Situations 1–4 reflect the output of the HWPP in the uncoordinated and the coordinated refill modes under various situations of reservoir and mean power output.

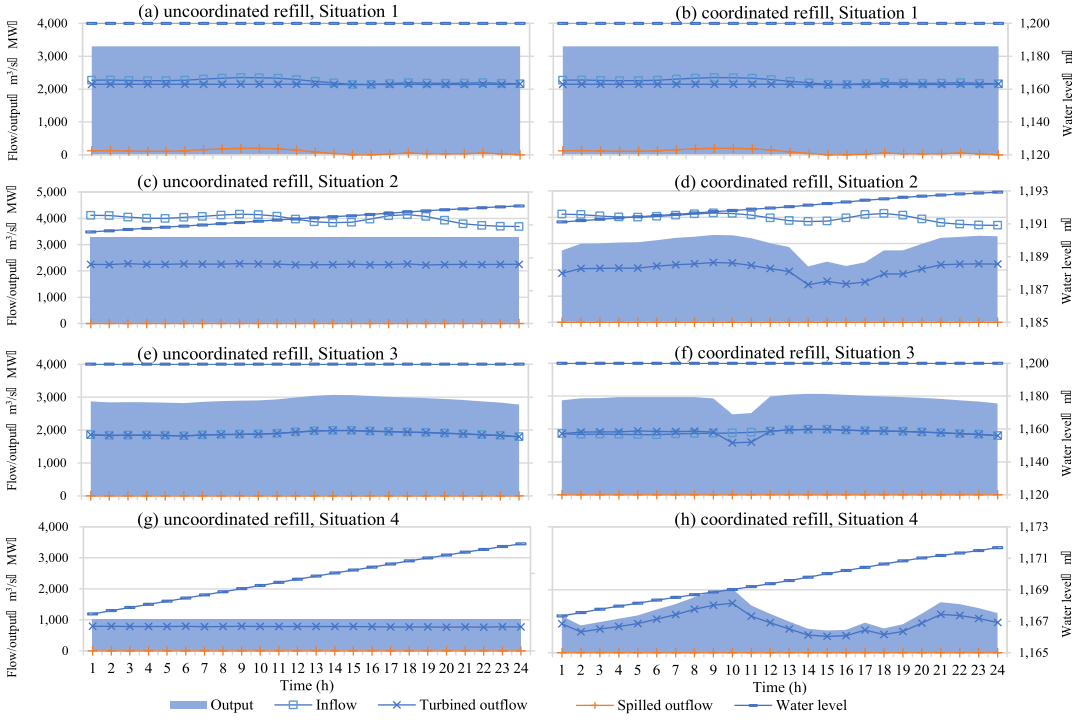

Fig. 13. Intraday operation of hydropower for Situations 1–4.

sources. This paper explores the operation of HWPP systems with large reservoirs during critical refill periods. First, during the scheduling phase, the proposed model employs a day-ahead optimal hourly operation of hydropower facilities that aims at simultaneously minimizing the fluctuation in the combined power output of these three resources and maximizing their power generation while adhering to the reservoir's water level and other common constraints. Then, during the operation phase, the prescribed scheduling is used as the input in a model that simulates the actual operations of the power system. The coordinated operation of the HWPP in this model not only dispatches the hydropower with a reciprocal output process to smooth the hourly fluctuation, but it also adjusts the hydropower output to achieve the target water level. The model is applied to a case study consisting of a large base of wind-photovoltaic-hydropower located in southwestern China. It compares the hourly operation of an HWPP in the uncoordinated mode and in the coordinated refill mode under three inflow

scenarios (dry, moderate, and wet). The results show that (1) with the proposed model, the hydropower operations effectively smooth the output fluctuation of the HWPP system without influencing the daily refill procedure; (2) when the reservoir is fully filled, the hydropower facility is still capable of smoothing the output fluctuation, but it incurs high losses in power production; (3) HWPP integration is more appropriate when the reservoir is not full and the hydropower output is below the installed capacity; and (4) when the reservoir is full, high spillage ($22\ m^3/s$–$402\ m^3/s$) and reductions in hydropower generation (0.1 GWh–11.4 GWh per day) suggest that the integration of the HWPP should be avoided.

Future work on the optimal operation of HWPP systems should be extended to other periods of the year (e.g., the preflood season or ecologically sensitive periods), which have complex constraints on the output shape, water level, discharge, and other aspects. Further potential impacts of multienergy source integration should be analyzed as well, such as the effects on the costs, reliability, air emissions, and other environmental metrics.

Declaration of Competing Interest

None.

Acknowledgments

The authors appreciate the contributions provided by Yiping Miao from Yalong River Hydropower Development Company, Ltd. and Shengbin Jiang from POWERCHINA Kunming Engineering Corporation Ltd.

The work of Xianxun Wang, Yadong Mei, and Hao Wang is supported by the Joint Funds of the National Natural Science Foundation of China [U1865201], the Program of the National Natural Science Foundation of China [51479140 and 91647204], and the Program of the Natural Science Youth Foundation of Hubei Province [ZRMS2017000495].

The work of Edgar Virguez is supported by the Alfred P. Sloan Foundation through the Duke University Energy Data Analytics Fellowship and by the CEIBA Foundation through the Rodolfo Llinas Scholarship. The work of Dalia Patiño-Echeverri is supported by the Center for Climate and Energy Decision Making [SES-0949710] funded by the National Science Foundation.

The work of Lihua Chen is supported by the National Key Research and Development Program of China [2017YFC0405900], the National Natural Science Foundation of China [51669003], and the Guangxi Provincial Natural Science Foundation [AB16380284].

The conclusions reached or positions taken by the researchers or other grantees represent the views of the grantees themselves and not those of the foundation or its trustees, officers, or staff.

Author contributions

Yadong Mei and Xianxun Wang conceived and designed the experiments; Xianxun Wang and Lihua Chen performed the investigation; Xianxun Wang executed the primary research simulation and analysis; Xianxun Wang and Edgar Virguez wrote the paper; Yadong Mei, Dalia Patiño-Echeverri, and Jordan Kern provide editorial advice for the paper; and Yadong Mei, Dalia Patiño-Echeverri, and Hao Wang supervised the research.

Appendix A

The data, software and parameters applied in this case study are displayed below.

(1) Data

All the data were obtained through communications with the operators and planners of a cascaded hydropower system in southwestern China and listed as tables and figures below. All the data displayed in the figures are also available upon request (See Table A.1, Figs. A.1, A.2, A.3, A.4 and A.5).

Table A.1
Parameters of the power stations.

Facility	Installed capacity (MW)	Normal water level (m)	Conservation storage ($10^6\ m^3$)	Dead water level (m)	Inactive storage ($10^6\ m^3$)
Hydropower	3300	1200	3370	1155	2420
Wind power	1000	–	–	–	–
PV power	2000	–	–	–	–

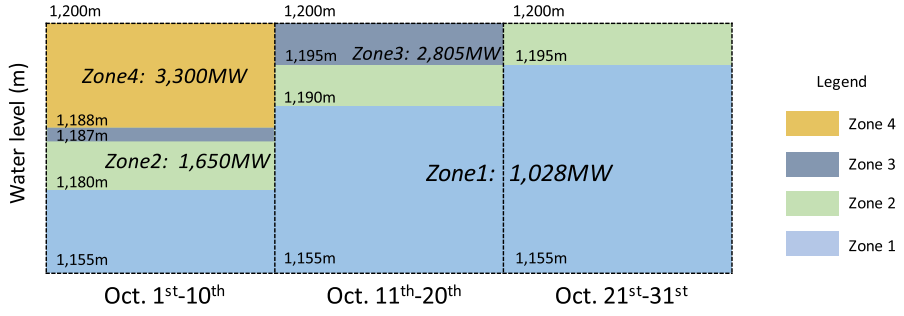

Fig. A.1. Operation rule curves for the reservoir: the reservoir is dispatched according to the zone decided by the water level and the date. In Zones 1, 2, 3, and 4, the power output of the reservoir are 1028 MW, 1650 MW, 2805 MW, and 3300 MW, respectively (If the water level is 1182 m at the beginning of October 5th, it is in Zone 2 and accordingly its power output is 1650 MW).

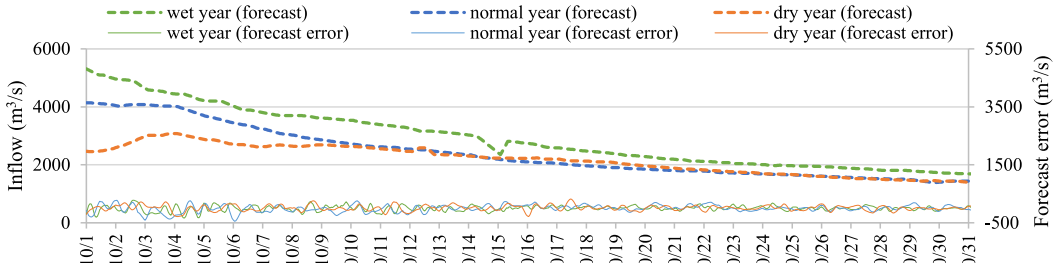

Fig. A.2. Inflow of hydropower (from 1:00 on October 1st to 24:00 on October 31st, source: POWERCHINA Kunming Engineering Corporation Ltd).

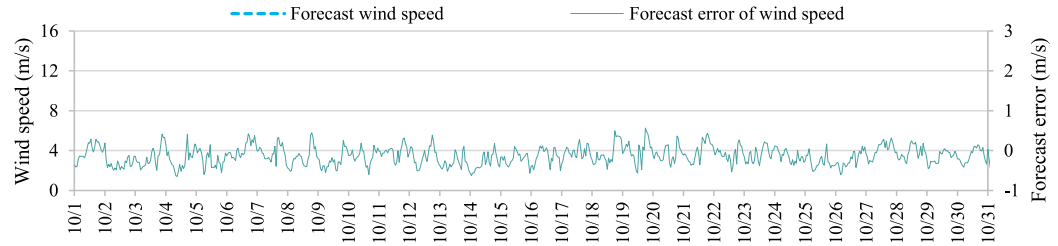

Fig. A.3. Wind speed of the wind farm (from 1:00 on October 1st 2011 to 24:00 on October 31st 2011, source: POWERCHINA Kunming Engineering Corporation Ltd).

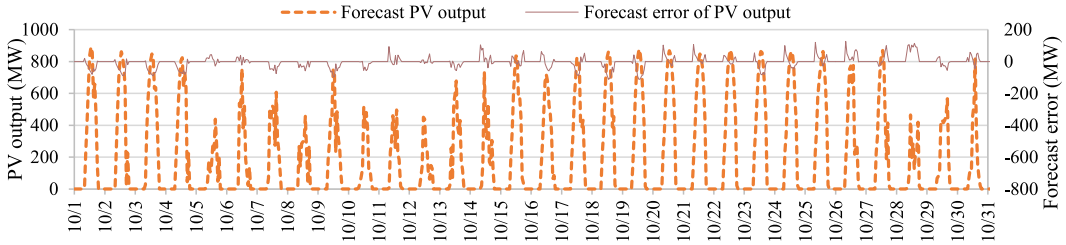

Fig. A.4. Output of the PV power station (from 1:00 on October 1st, 2015 to 24:00 on October 31st, 2015, source: POWERCHINA Kunming Engineering Corporation Ltd).

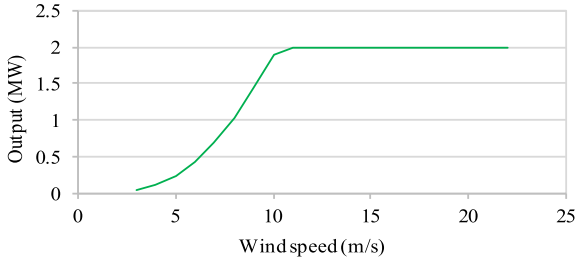

Fig. A.5. Wind turbine power curve (the rated capacity is 2 MW, source: POWERCHINA Kunming Engineering Corporation Ltd).

The day-ahead, forecast error of the inflow, wind speed, and solar radiation is assumed to be a random variable that was independent and identically distributed (See Figs. A.2, A.3, and A.4). It is expressed as a percentage of the forecast and follows a standard normal probability distribution (i.e., with a mean of zero and a standard deviation of one). In addition, there are other assumptions or simplifications, including the start date of refill period, the constraint of the power grid, and the temporal scale of the integration. These assumptions are helpful for solving the optimization model efficiently. Because the characteristics of the system most likely to affect the HWPP operations during the refill period (e.g., the

uncertainty and variability of the wind and PV power, the flexibility of hydropower, and the procedure for refilling the reservoir) must be maintained, the conclusions are unlikely to be affected by these assumptions.

(2) Software and parameters

The scheduling model is solved in MATLAB using the NSGA-II method, a tool for multiobjective optimization. As mentioned, the NSGA-II parameters used were as follows: 100 as the population size, 0.5 as the crossover rate, 0.01 as the mutation rate, and 50 as the generation number. Other parameters, such as the crossover type, mutation type and selection type, were left equal to their default values.

Alternative optimization methods (e.g., Particle Swarm Optimization) and software (e.g., Python) could have been used to solve the multiobjective model proposed here. While the computing time and exact values of the variables obtained using different techniques and parameters could have been different, the overall results should be similar and should not affect the conclusions.

Appendix B

The Pareto frontier solutions under Scenarios 1, 2, and 3 are displayed in Figs. B.1, B.2, and B.3 respectively.

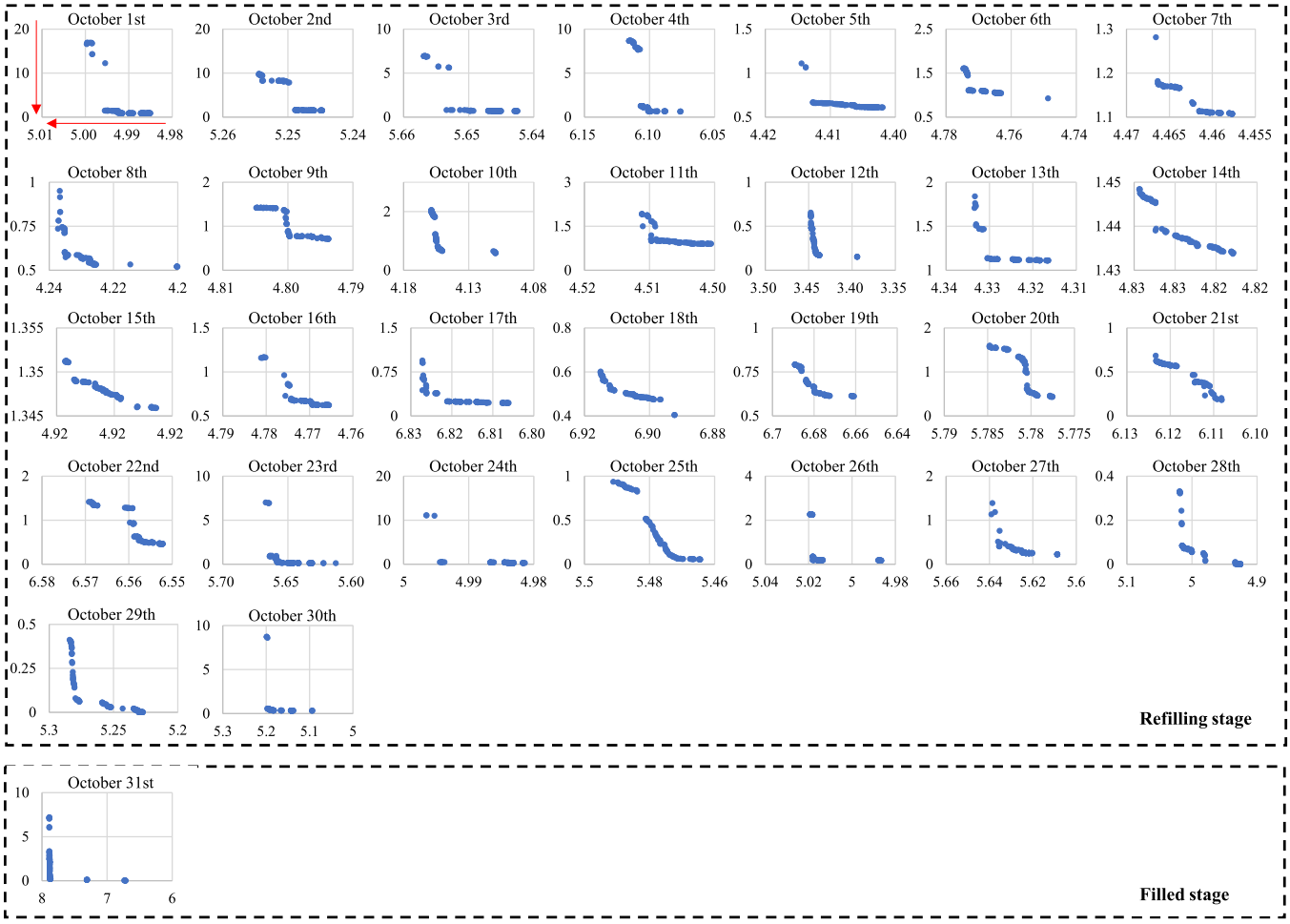

Fig. B.1. Pareto frontier solution for the multiobjective optimization of HWPP integration under Scenario 1: the abscissa is the power generation, the unit of which is 10 GWh; the ordinate is the output fluctuation, the unit of which is 10 GW; and the red arrow points to the preferred value of the objective, which is similar hereafter.

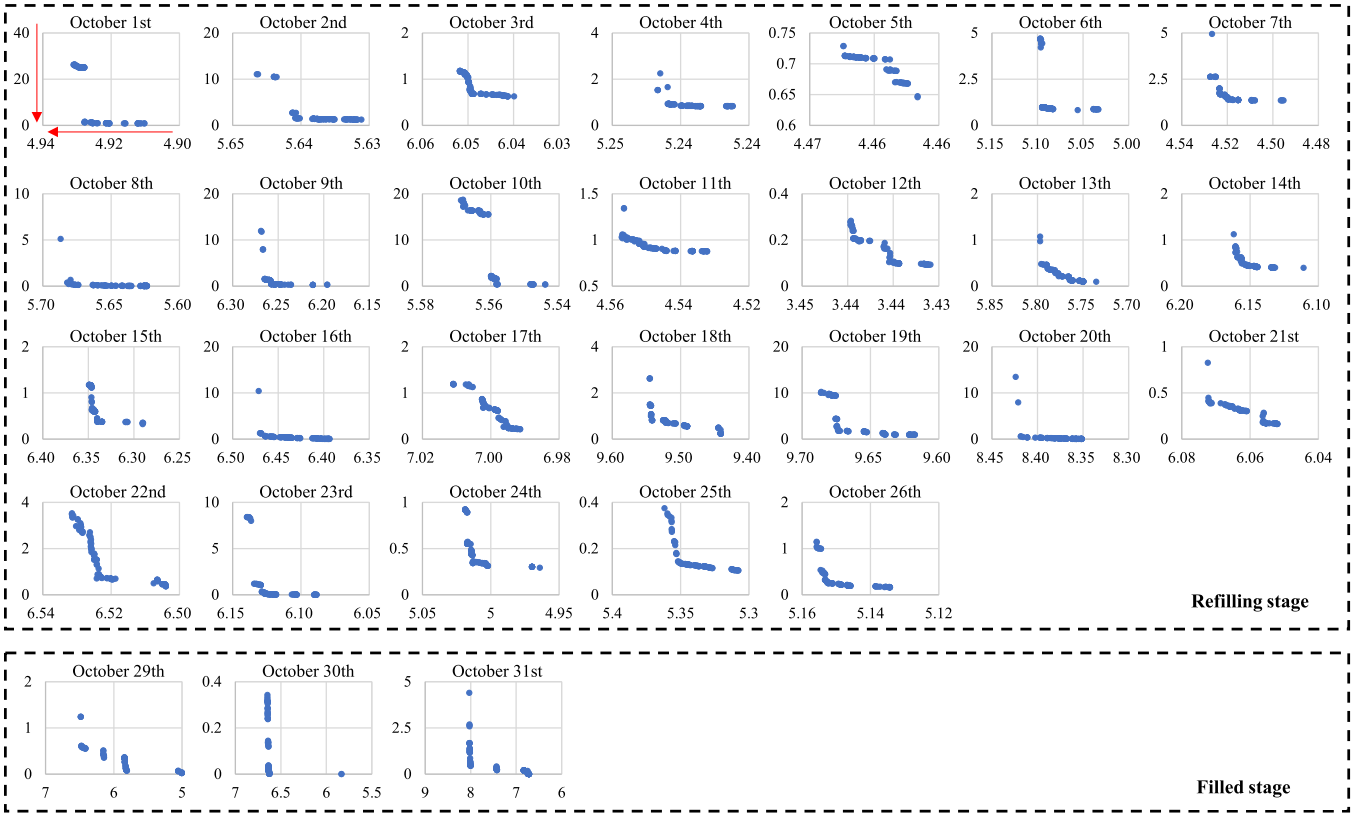

Fig. B.2. Pareto frontier solution of multiobjective optimization for HWPP integration under Scenario 2.

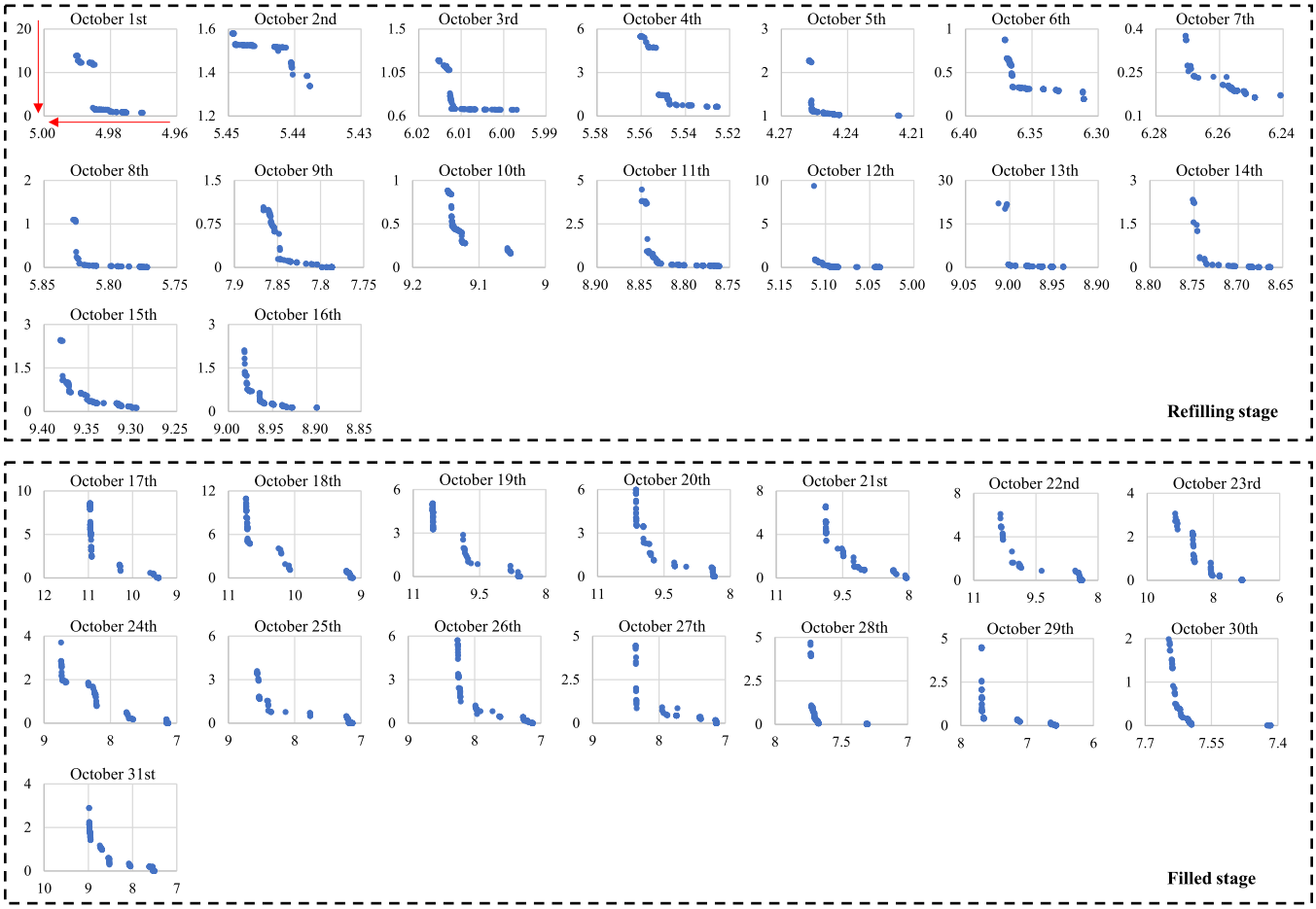

Fig. B.3. Pareto frontier solution of multiobjective optimization for HWPP integration under Scenario 3.

References

[1] Francois B, Borga M, Anquetin S, Creutin JD, Engeland K, Favre AC, et al. Integrating hydropower and intermittent climate-related renewable energies: a call for hydrology. Hydrol Process 2014;28:5465–8. https://doi.org/10.1002/hyp.10274.

[2] Jacobson MZ, Delucchi MA, Cameron MA, Frew BA. Low-cost solution to the grid reliability problem with 100% penetration of intermittent wind, water, and solar for all purposes. Proc Natl Acad Sci USA 2015;112:15060–5. https://doi.org/10.1073/pnas.1510028112.

[3] Ahmad A, El-Shafie A, Razali SFM, Mohamad ZS. Reservoir optimization in water resources: a review. Water Resour Manage 2014;28:3391–405. https://doi.org/10.1007/s11269-014-0700-5.

[4] Cunderlik JM, Ouarda T, Bobee B. On the objective identification of flood seasons. Water Resour Res 2004;40. https://doi.org/10.1029/2003wr002295.

[5] Fang W, Huang Q, Huang S, Yang J, Meng E, Li Y. Optimal sizing of utility-scale photovoltaic power generation complementarily operating with hydropower: a case study of the world's largest hydro-photovoltaic plant. Energy Convers Manage 2017;136:161–72. https://doi.org/10.1016/j.enconman.2017.01.012.

[6] Tahseen S, Karney BW. Reviewing and critiquing published approaches to the sustainability assessment of hydropower. Renew Sustain Energy Rev 2017;67:225–34. https://doi.org/10.1016/j.rser.2016.09.031.

[7] Ming B, Liu P, Guo S, Zhang X, Feng M, Wang X. Optimizing utility-scale photovoltaic power generation for integration into a hydropower reservoir by incorporating long- and short-term operational decisions. Appl Energy 2017;204:432–45. https://doi.org/10.1016/j.apenergy.2017.07.046.

[8] Kern JD, Patino-Echeverri D, Characklis GW. An integrated reservoir-power system model for evaluating the impacts of wind integration on hydropower resources. Renew Energy 2014;71:553–62. https://doi.org/10.1016/j.renene.2014.06.014.

[9] Wang XB, Chang JX, Meng XJ, Wang YM. Short-term hydro-thermal-wind-photovoltaic complementary operation of interconnected power systems. Appl Energy 2018;229:945–62. https://doi.org/10.1016/j.apenergy.2018.08.034.

[10] Ming B, Liu P, Cheng L, Zhou YL, Wang XX. Optimal daily generation scheduling of large hydro-photovoltaic hybrid power plants. Energy Convers Manage 2018;171:528–40. https://doi.org/10.1016/j.enconman.2018.06.001.

[11] Segurado R, Madeira JFA, Costa M, Duić N, Carvalho MG. Optimization of a wind powered desalination and pumped hydro storage system. Appl Energy 2016;177:487–99. https://doi.org/10.1016/j.apenergy.2016.05.125.

[12] Wang X, Mei Y, Kong Y, Lin Y, Wang H. Improved multi-objective model and analysis of the coordinated operation of a hydro-wind-photovoltaic system. Energy 2017;134:813–39. https://doi.org/10.1016/j.energy.2017.06.047.

[13] Jurasz J, Mikulik J, Krzywda M, Ciapała B, Janowski M. Integrating a wind- and solar-powered hybrid to the power system by coupling it with a hydroelectric power station with pumping installation. Energy 2018;144:549–63. https://doi.org/10.1016/j.energy.2017.12.011.

[14] Ma T, Yang H, Lu L, Peng J. Optimal design of an autonomous solar-wind-pumped storage power supply system. Appl Energy 2015;160:728–36. https://doi.org/10.1016/j.apenergy.2014.11.026.

[15] Kern JD, Patino-Echeverri D, Characklis GW. The impacts of wind power integration on sub-daily variation in river flows downstream of hydroelectric dams. Environ Sci Technol 2014;48:9844–51. https://doi.org/10.1021/es405437h.

[16] Liu P, Guo SL, Xiong LH, Chen L. Flood season segmentation based on the probability change-point analysis technique. Hydrol Sci J Des Sci Hydrol 2010;55:540–54. https://doi.org/10.1080/02626667.2010.481087.

[17] Chen L, Singh VP, Guo SL, Zhou JZ, Zhang JH, Liu P. An objective method for partitioning the entire flood season into multiple sub-seasons. J Hydrol 2015;528:621–30. https://doi.org/10.1016/j.jhydrol.2015.07.003.

[18] Liu P, Guo SL, Xiong LH, Li W, Zhang HG. Deriving reservoir refill operating rules by using the proposed DPNS model. Water Resour Manage 2006;20:337–57. https://doi.org/10.1007/s11269-006-0322-7.

[19] Zhou YL, Guo SL, Xu CY, Liu P, Qin H. Deriving joint optimal refill rules for cascade reservoirs with multi-objective evaluation. J Hydrol 2015;524:166–81. https://doi.org/10.1016/j.jhydrol.2015.02.034.

[20] Li Y, Guo SL, Quo JL, Wang Y, Li TY, Chen JH. Deriving the optimal refill rule for multi-purpose reservoir considering flood control risk. J Hydro-Environ Res 2014;8:248–59. https://doi.org/10.1016/j.jher.2013.09.005.

[21] Xie AL, Liu P, Guo SL, Zhang XQ, Jiang H, Yang G. Optimal design of seasonal flood limited water levels by jointing operation of the reservoir and floodplains. Water Resour Manage 2018;32:179–93. https://doi.org/10.1007/s11269-017-1802-7.

[22] Liu XY, Guo SL, Liu P, Chen L, Li XA. Deriving optimal refill rules for multi-purpose reservoir operation. Water Resour Manage 2011;25:431–48. https://doi.org/10.1007/s11269-010-9707-8.

[23] Cheng CT, Shen JJ, Wu XY, Chau KW. Operation challenges for fast-growing China's hydropower systems and respondence to energy saving and emission reduction. Renew Sustain Energy Rev 2012;16:2386–93. https://doi.org/10.1016/j.rser.2012.01.056.

[24] Zhou YL, Guo SL, Chang FJ, Liu P, Chen AB. Methodology that improves water utilization and hydropower generation without increasing flood risk in mega cascade reservoirs. Energy 2018;143:785–96. https://doi.org/10.1016/j.energy.2017.11.035.

[25] REN21. Renewables 2017 Global Status Report, http://www.ren21.net/gsr-2017/; 2018 (accessed 15.01.19).

[26] Li X, Chen Z, Fan X, Cheng Z. Hydropower development situation and prospects in China. Renew Sustain Energy Rev 2018;82:232–9. https://doi.org/10.1016/j.rser.2017.08.090.

[27] X.N. Agency. First clean energy base of wind-PV-hydro integration over the basin in China will be built in Yalong River basin (in Chinese), http://www.xinhuanet.com/2016-03/27/c_1118454757.htm; 2016 (accessed 10.11.18).

[28] Deb K, Agrawal S, Pratap A, Meyarivan T. A Fast Elitist Non-dominated Sorting Genetic Algorithm for Multi-objective Optimization: NSGA-II. Lect Notes Comput Sci 2000;2000:849–58. https://doi.org/10.1007/3-540-45356-3_83.

[29] Wang X, Mei Y, Cai H, Cong X. A new fluctuation index: Characteristics and application to hydro-wind systems. Energies 2016;9:1–17. https://doi.org/10.3390/en9020114.

[30] Baker DB, Richards RP, Loftus TT, Kramer JW. A new flashiness index: characteristics and applications to midwestern rivers and streams. J Am Water Resour Assoc 2004;40:503–22. https://doi.org/10.1111/j.1752-1688.2004.tb01046.x.

[31] Gao JJ, Zheng Y, Li JM, Zhu XM, Kan K. Optimal Model for complementary operation of a photovoltaic-wind-pumped storage system. Math Prob Eng 2018. https://doi.org/10.1155/2018/5346253.

[32] Sterl S, Liersch S, Koch H, van Lipzig NPM, Thiery W. A new approach for assessing synergies of solar and wind power: implications for West Africa. Environ Res Lett 2018;13. https://doi.org/10.1088/1748-9326/aad8f6.

[33] Zhang XS, Ma GW, Huang WB, Chen SJ, Zhang S. Short-term optimal operation of a wind-pv-hydro complementary installation: yalong river, sichuan province. chinaEnergies 2018;11. https://doi.org/10.3390/en11040868.

[34] Wang X, Chen L, Chen Q, Mei Y, Wang H. Model and analysis of integrating wind and pv power in remote and core areas with small hydropower and pumped hydropower storage. Energies 2018;11:3459. https://doi.org/10.3390/en11123459.

[35] Su YF, Kern JD, Characklis GW. The impact of wind power growth and hydrological uncertainty on financial losses from oversupply events in hydropower-dominated systems. Appl Energy 2017;194:172–83. https://doi.org/10.1016/j.apenergy.2017.02.067.

[36] C.C. Coutant, R. Mann, M.J. Sale. Reduced spill at hydropower dams: opportunities for more generation and increased fish population. Oak Ridge National Laboratory, Oak Ridge, Tennessee, 2006. doi: 10.2172/974617.

[37] Liu BX, Cheng CT, Wang S, Liao SL, Chau KW, Wu XY, et al. Parallel chance-constrained dynamic programming for cascade hydropower system operation. Energy 2018;165:752–67. https://doi.org/10.1016/j.energy.2018.09.140.

[38] Yuan XH, Tian H, Yuan YB, Huang YH, Ikram RM. An extended NSGA-III for solution multi-objective hydro-thermal-wind scheduling considering wind power cost. Energy Convers Manage 2015;96:568–78. https://doi.org/10.1016/j.enconman.2015.03.009.

[39] Seshadri A. NSGA - II: A multi-objective optimization algorithm. Implementierung: MAT-Lab Central; 2009.

[40] Intakes COH. Glossary of hydropower terms. Guidelines for design of intakes for hydroelectric plants. ASCE Lib 2014. https://doi.org/10.1061/9780784400739.bm.

[41] Taormina R, Chau KW, Sivakumar B. Neural network river forecasting through baseflow separation and binary-coded swarm optimization. J Hydrol 2015;529:1788–97. https://doi.org/10.1016/j.jhydrol.2015.08.008.

[42] Moazenzadeh R, Mohammadi B, Shamshirband S, Chau KW. Coupling a firefly algorithm with support vector regression to predict evaporation in northern Iran. Eng Appl Comp Fluid Mech 2018;12:584–97. https://doi.org/10.1080/19942060.2018.1482476.

[43] Chau KW. Use of meta-heuristic techniques in rainfall-runoff modelling. Water 2017;9. https://doi.org/10.3390/w9030186.

[44] Yaseen ZM, Sulaiman SO, Deo RC, Chau KW. An enhanced extreme learning machine model for river flow forecasting: State-of-the-art, practical applications in water resource engineering area and future research direction. J Hydrol 2019;569:387–408. https://doi.org/10.1016/j.jhydrol.2018.11.069.

[45] Zou P, Chen QX, Yu Y, Xia Q, Kang CQ. Electricity markets evolution with the changing generation mix: an empirical analysis based on China 2050 High Renewable Energy Penetration Roadmap. Appl Energy 2017;185:56–67. https://doi.org/10.1016/j.apenergy.2016.10.061.

[46] Cornelius A, Bandyopadhyay R, Patiño-Echeverri D. Assessing environmental, economic, and reliability impacts of flexible ramp products in MISO's electricity market. Renew Sustain Energy Rev 2018;81:2291–8. https://doi.org/10.1016/j.rser.2017.06.037.